Information Sciences Letters
An International Journal
http://dx.doi.org/10.18576/isl/050201

Effects of Second Order Chemical Reaction on MHD Free Convection Dissipative Fluid Flow past an Inclined Porous Surface by way of Heat Generation: A Lie Group Analysis

M. Y. Malik and Khalil-ur-Rehman[*]

Department of Mathematics, Quaid-i-Azam University Islamabad 44000, Pakistan.

Received: 21 Feb. 2016, Revised: 20 Apr. 2016, Accepted: 24 Apr. 2016.
Published online: 1 May 2016.

Abstract: In this paper, an analysis has been made to explore the characteristics of second order chemical reaction on steady two-dimensional MHD flow of electrically conducting, viscous incompressible fluid in a porous media with heat and mass transfer. A role of free convection is explored by considering viscous dissipation term in energy equation. The symmetry groups admitted by governing boundary value problem are obtained via Lie algebra. The corresponding Lie's scaling group of transformations are used to convert coupled non-linear partial differential equations into non-linear ordinary differential equations. Consequently, numerical solution of these equations are investigated by using fifth order R-K (Runge-Kutta) algorithm with shooting technique. The present study revealed that the dimensionless temperature variation is on a serious node against heat generation parameter. Furthermore, effect logs of velocity, temperature and concentration distribution aimed at different physical parameters are discussed graphically. Numerical values of skin friction, Nusselt and Sherwood numbers against various embedded parameters are validated by favourable comparison with previously published results.

Keywords: Lie group analysis, MHD flow, Porous medium, Natural convection, Viscous dissipation, Heat generation, Chemical reaction.

1 Introduction

Integration theory for differential equations was proposed by Norwegian mathematician Sophus Lie in early nineteenth century and has played a central role regarding mathematical traits of solution system governed by continuous differential equations. Lie group analysis generally called as Lie symmetry analysis was established to find out continuous point transformations which map a concerning differential equation to itself. By using symmetry analysis we can clip all symmetries of given differential equations without prior knowledge of equations and ad hoc assumptions. Whereas, Lie's scaling transformation is used to obtain invariants, similarity solutions, solution integrals, to mention just a few [1]-[4]. Mostly the non-linear character of differential equations made task hard to trace out the solution of physical problems. So, many researchers in this frame of interest are still busy to search out the similarity solutions especially in the field of fluid mechanics. As far as scaling point group of transformations are concern, the group invariant solutions are nothing but the well familiar similarity solutions [5]. Since the Prandtl's boundary layer equations admits number of distinct symmetry groups therefore, several attempts has been made to study physical phenomena's like Yurusoy and Pakdemirli [6] identified symmetry reductions for three dimensional unsteady non-Newtonian fluids flow. Kalpakides and Balassas [7] studied the boundary layer fluid flow over an elastic surface by utilizing group theoretic approach. Hassan *et al.* [8] deliberated the variable viscosity effects of MHD boundary layer fluid flow due to stretching sheet by way of Lie group. Sivansankaran *et al.* [9] investigated the heat and mass diffusion of natural convection fluid flow over an inclined surface by using Lie group approach.

Plasma theory, nuclear reactors, MHD electrolysis designs, MHD generators, glass manufacturing and paper productions are the practical works corresponds to magneto-hydrodynamic flow of an electrically conducting fluid. The purification process of melted metals from non-metallic inclusions demands different hydro-magnetic techniques and careful use of magnetic field. Further, MHD free convection fluid flows claims several noteworthy applications in the area of aeronautical plasma, electronics, planetary magneto-spheres and chemical engineering cite. Thus such type of viscous flow problems with which we are dealing, is much more useful. Petroleum engineering, industrial filtration, water purification, storage of vegetables and fruits, solid matrix heat exchangers and nuclear waste give rise to the study of heat transfer by convection through surfaces which are embedded in a porous media. Whereas, the combined diffusion of mass and heat against involved geometries embedded in a porous media has vast geophysical and engineering applications like cooling of nuclear reactor,

[*]Corresponding author e-mail: krehman@math.qau.edu.pk

drying of porous solids, enhanced oil recovery and underground energy transportation etc. Beithou *et al.* [10] considered the free convection flow with porosity effect adjacent to vertical plate surrounded by porous medium. The natural convection flow past over a porous inclined surface was taken by Chen [11]. Devi and Ganga [12] explored the viscous dissipation effect on nonlinear MHD flow along a stretching porous surface. The concept of simultaneous heat and mass diffusion have received significant intensions regarding practical interest in engineering areas like polymer solution, wet-bulb thermometer and food processing etc. Several solutions of viscoelastic fluid by considering MHD slip flow along a stretching sheet was proposed by Turkyilmazoglu [13]. Subhashini *et al.* [14] explored the simultaneous influence of heat and mass diffusions with mixed convection boundary layer flow past a porous surface along convective surface endpoint conditions. Heat analysis of Eyring-Powell fluid flow over a continuously moving surface with convective endpoint conditions was identified by Hayat *et al.* [15]. Reddy *et al.* [16] considered heat and mass diffusion effects on free convection dissipative, steady MHD fluid flow past over an inclined porous surface. Heat analysis regarding viscous dissipative fluid flow along a vertical plate by means of induced magnetic field was taken by Raju *et al.* [17].

There are different types of reactions namely, endothermic, exothermic, homogeneous and heterogeneous. They may be first or higher order. Solar collectors, nuclear reactor safety and combustion system to mention just a few includes the transporting process, which are directed by coupled action of buoyancy forces due to both heat and mass transfer under high order chemical reaction effects. A species molecular diffusion with chemical reaction in or at the boundary involves number of concrete diffusive operations and still a topic of great interest. The effect logs of thermal stratification, chemical reaction by way of heat source along a stretching sheet was studied by Kandasamy *et al.* [18]. Mingchun *et al.* [19] considered the influence of strong endothermic chemical reaction under non-thermal equilibrium flow model of porous medium. Thermally stratified flow along a stretching surface with chemical reaction and heat source was taken by Kishan and Amrutha [20]. Kandasamy *et al.* [21] identified the free convective heat and mass transfer fluid flow past a stretching surface with chemical reaction and thermophoresis effect by using group theory. The first order homogeneous chemical reaction effects on two dimensional boundary layer flow over a vertical stretching surface was numerically examined by Makinde and Sibanda [22]. Tripathy *et al.* [23] considered chemical reaction impacts on free convection MHD fluid flow past a moving vertical permeable plate. The effect logs of chemical reaction on a boundary layer flow through a linearly stretching sheet with heat mass transfer effect was studied by Ferdows *et al.* [24].

The above literature survey shows that most of the investigations are made against lower order chemical reactions and reveals that as yet, no study has been testified on MHD two dimensional incompressible dissipative boundary layer fluid flow with heat and mass transfer over a porous media under high order chemical reaction by means of heat generation effect. Therefore, the aim of our analysis is to extend the work of Reddy *et al.* [25] by considering high order chemical reaction with heat generation effect Application of Lie algebra reduced the system of coupled non-linear partial differential equations into a system of coupled non-linear ordinary differential equations by dropping independents. This system remains invariant under defined relation among the parameters of transformations. Furthermore, these transformed equations are solved with the aid of fifth order Runge-Kutta algorithm with shooting technique and results so obtained are in good agreement with previously published results of Reddy *et al.* [25].

2 Flow analysis

Consider steady two-dimensional hydro-magnetic incompressible electrically conducting laminar flow of a viscous dissipating fluid past over a semi-infinite acutely inclined plate embedded in a porous media with manifestation of chemically reactive species (undergoing a second order chemical reaction). It is made-up that the fluid flow is along $\tilde{x}-\text{axis}$ and $\tilde{y}-\text{axis}$ is normal to it. Influence of an induced magnetic field is ignored due to assumption taken into account that the magnetic Reynolds number is considerably less than unity.

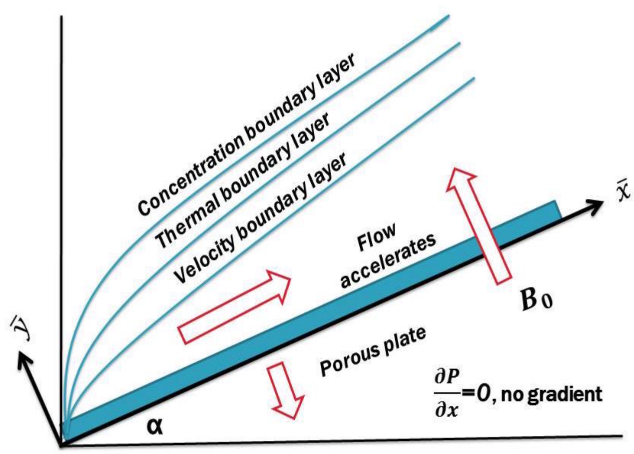

Fig. 1(a). Schematic diagram of the flow model.

The fluid properties are considered to be constant except the effects of density variation under temperature and concentration. Temperature difference is developed by maintaining surface at temperature $\tilde{T}_w$, which is higher than the $\tilde{T}_\infty$ (constant temperature) of the surrounding fluid and concentration $\tilde{C}_w$ is greater than the $\tilde{C}_\infty$ (constant concentration) . In the present analysis, Soret and Dufour effects are unimportant because foreign mass concentration level is supposed to be low. The governing mass, momentum, energy and mass concentration equations of this flow model under the usual boundary layer and Boussinesq's approximations are given by:

$$\frac{\partial \tilde{u}}{\partial \tilde{x}}+\frac{\partial \tilde{v}}{\partial \tilde{y}}=0, \tag{1}$$

$$\tilde{u}\frac{\partial \tilde{u}}{\partial \tilde{x}}+\tilde{v}\frac{\partial \tilde{u}}{\partial \tilde{y}}=\nu\frac{\partial^2 \tilde{u}}{\partial \tilde{y}^2}+g\beta_T(\tilde{T}-\tilde{T}_\infty)\cos\alpha+g\beta_C(\tilde{C}-\tilde{C}_\infty)\cos\alpha-\frac{\sigma B_0^2}{\rho}\tilde{u}-\frac{\nu\tilde{u}}{K_p}, \tag{2}$$

$$\tilde{u}\frac{\partial \tilde{T}}{\partial \tilde{x}}+\tilde{v}\frac{\partial \tilde{T}}{\partial \tilde{y}}=\frac{\kappa}{\rho c_p}\frac{\partial^2 \tilde{T}}{\partial \tilde{y}^2}+\frac{\mu}{\rho c_p}(\frac{\partial \tilde{u}}{\partial \tilde{y}})^2+\frac{Q_0(\tilde{T}-\tilde{T}_\infty)}{\rho c_p}, \tag{3}$$

$$\tilde{u}\frac{\partial \tilde{C}}{\partial \tilde{x}}+\tilde{v}\frac{\partial \tilde{C}}{\partial \tilde{y}}=D\frac{\partial^2 \tilde{C}}{\partial \tilde{y}^2}-K_r(\tilde{C}-\tilde{C}_\infty)^m, \tag{4}$$

where $(\tilde{u},\tilde{v})$ denotes components of the velocity in the $(\tilde{x},\tilde{y})$ directions, $\nu=\frac{\mu}{\rho}$, g, β_T, $\tilde{T}$, $\tilde{T}_\infty$, β_C, $\tilde{C}$, $\tilde{C}_\infty$, ρ, σ, B_0, K_p, k, c_p, μ, Q_0, D, K_r, and m is the kinematic viscosity, gravitational acceleration, thermal expansion coefficient, temperature in the boundary layer, fluid temperature far away from the surface, concentration expansion coefficient, species concentration in the boundary layer, species concentration in the fluid far away from the surface, fluid density, fluid electrical conductivity, applied magnetic field strength, permeability of the porous medium, thermal conductivity of the fluid, specific heat at constant pressure, viscosity coefficient, heat generation constant, mass diffusivity, chemical reaction rate constant and order of chemical reaction respectively. The boundary conditions at the plate and far away from surface are prescribed as:

$$\tilde{u}=0,\ \ \tilde{v}=0,\ \ \tilde{T}=\tilde{T}_w,\ \ \tilde{C}=\tilde{C}_w\ \ at\ \ \tilde{y}=0,$$

$$\tilde{u}\to 0,\ \ \tilde{T}\to\tilde{T}_\infty,\ \ \tilde{C}\to\tilde{C}_\infty,\ \ as\ \ \tilde{y}\to\infty. \tag{5}$$

Proceeding with analysis, we introduce a non-dimensional quantities

$$x=\frac{\tilde{x}U_\infty}{\nu},\ y=\frac{\tilde{y}U_\infty}{\nu},\ u=\frac{\tilde{u}}{U_\infty},\ v=\frac{\tilde{v}}{U_\infty},\ M=\frac{\sigma B_0^2\nu}{U_\infty^3},\ \Pr=\frac{\nu}{\alpha},\ Sc=\frac{\nu}{D},$$

$$Gr=\frac{\nu g\beta_T\left(\tilde{T}_w-\tilde{T}_\infty\right)}{U_\infty^3},\ Gm=\frac{\nu g\beta_C\left(\tilde{C}_w-\tilde{C}_\infty\right)}{U_\infty^3},\ \theta=\frac{\tilde{T}-\tilde{T}_\infty}{\tilde{T}_w-\tilde{T}_\infty},\ \phi=\frac{\tilde{C}-\tilde{C}_\infty}{\tilde{C}_w-\tilde{C}_\infty}, \tag{6}$$

$$Ec=\frac{U_\infty^2}{c_p(\tilde{T}_w-\tilde{T}_\infty)},\ K=\frac{K_pU_\infty^3}{\nu^3},\ Cr=\frac{K_r\nu(\tilde{C}_w-\tilde{C}_\infty)^m}{U_\infty^2(\tilde{C}_w-\tilde{C}_\infty)},\ Q=\frac{Q_0\nu}{\rho c_p U_\infty^2},$$

Incorporating Eq. (6) into Eqs. (1)-(4), we get

$$\frac{\partial u}{\partial x}+\frac{\partial v}{\partial y}=0, \tag{7}$$

$$u\frac{\partial u}{\partial x}+v\frac{\partial u}{\partial y}=\frac{\partial^2 u}{\partial y^2}+Gr\theta\cos\alpha+Gm\phi\cos\alpha-(M+\frac{1}{K})u, \tag{8}$$

$$u\frac{\partial \theta}{\partial x}+v\frac{\partial \theta}{\partial y}=\frac{1}{\Pr}\frac{\partial^2\theta}{\partial y^2}+Ec(\frac{\partial u}{\partial y})^2+Q\theta, \tag{9}$$

$$u\frac{\partial \phi}{\partial x}+v\frac{\partial \phi}{\partial y}=\frac{1}{Sc}\frac{\partial^2\phi}{\partial y^2}-Cr\phi^m, \tag{10}$$

the resultant boundary conditions are

$$u=0,\ v=0,\ \theta=1,\ \phi=1\ at\ \ y=0,$$

$$u\to 0,\ \theta\to 0,\ \phi\to 0\ \ as\ \ y\to\infty. \tag{11}$$

By using velocity components in terms of stream function $\bar{\Psi}$ as:

$$u=\frac{\partial\bar{\Psi}}{\partial y}, v=-\frac{\partial\bar{\Psi}}{\partial x},$$

So that, the Eqs. (8)-(10) reduces to

$$(\frac{\partial\bar{\Psi}}{\partial y}\frac{\partial^2\bar{\Psi}}{\partial x\partial y}-\frac{\partial\bar{\Psi}}{\partial x}\frac{\partial^2\bar{\Psi}}{\partial y^2})=\frac{\partial^3\bar{\Psi}}{\partial y^3}+Gr\theta\cos\alpha+Gm\phi\cos\alpha-(M+\frac{1}{K})\frac{\partial\bar{\Psi}}{\partial y}, \tag{12}$$

$$(\frac{\partial\bar{\Psi}}{\partial y}\frac{\partial\theta}{\partial x}-\frac{\partial\bar{\Psi}}{\partial x}\frac{\partial\theta}{\partial y})=\frac{1}{\Pr}\frac{\partial^2\theta}{\partial y^2}+Ec(\frac{\partial^2\bar{\Psi}}{\partial y^2})^2+Q\theta, \tag{13}$$

$$(\frac{\partial\bar{\Psi}}{\partial y}\frac{\partial\phi}{\partial x}-\frac{\partial\bar{\Psi}}{\partial x}\frac{\partial\phi}{\partial y})=\frac{1}{Sc}\frac{\partial^2\phi}{\partial y^2}-K_r\phi^m, \tag{14}$$

the reduced boundary conditions takes the form

$$\frac{\partial\bar{\Psi}}{\partial y}=0,\ \frac{\partial\bar{\Psi}}{\partial x}=0,\ \theta=1,\ \phi=1\ \ at\ \ y=0,$$

$$\frac{\partial\bar{\Psi}}{\partial y}\to 0,\ \theta\to 0,\ \phi\to 0\ \ as\ \ y\to\infty. \tag{15}$$

To find out the solution of Eqs. $(12)-(14)$ is same as to determine the invariant solutions under a particular continuous one parameter group. We are looking for transformations group from a elementary set of one parameter scaling transformations. So, Lie-group transformations (Reddy *et al.* [25]) are given by:

$$\Gamma:\ x^*=xe^{\varepsilon\xi_1},\ y^*=ye^{\varepsilon\xi_2},\ \bar{\Psi}^*=\bar{\Psi}e^{\varepsilon\xi_3},\ u^*=ue^{\varepsilon\xi_4},\ v^*=ve^{\varepsilon\xi_5},\ \theta^*=\theta e^{\varepsilon\xi_6},\ \phi^*=\phi e^{\varepsilon\xi_7}, \tag{16}$$

Here ξ_1, ξ_2, ξ_3, ξ_4, ξ_5, ξ_6 and ξ_7 denotes transformation parameters and ε is a small parameter. The point-transformations Eq. (16) reduces the coordinates $(x, y, \bar{\Psi}, u, v, \theta, \phi)$ into new coordinates $(x^*, y^*, \bar{\Psi}^*, u^*, v^*, \theta^*, \phi^*)$. Now substituting Eq. (16) in Eqs. (12)-(14), we find that

$$e^{\varepsilon(\xi_1+2\xi_2-2\xi_3)}\left(\frac{\partial\bar{\Psi}^*}{\partial y^*}\frac{\partial^2\bar{\Psi}^*}{\partial x^*\partial y^*}-\frac{\partial\bar{\Psi}^*}{\partial x^*}\frac{\partial^2\bar{\Psi}^*}{\partial y^{*2}}\right)=\left[\begin{array}{l} e^{\varepsilon(3\xi_2-\xi_3)}\frac{\partial^3\bar{\Psi}^*}{\partial y^{*3}}+e^{-\varepsilon\xi_6}Gr\theta\cos\alpha+ \\ e^{-\varepsilon\xi_7}Gm\phi\cos\alpha-e^{\varepsilon(\xi_2-\xi_3)}(M+\frac{1}{K})\frac{\partial\bar{\Psi}^*}{\partial y^*}\end{array}\right], \tag{17}$$

$$e^{\varepsilon(\xi_1+\xi_2-\xi_3-\xi_6)}\left(\frac{\partial\bar{\Psi}^*}{\partial y^*}\frac{\partial\theta^*}{\partial x^*}-\frac{\partial\bar{\Psi}^*}{\partial x^*}\frac{\partial\theta^*}{\partial y^*}\right)=e^{\varepsilon(2\xi_2-\xi_6)}\frac{1}{\Pr}\frac{\partial^2\theta^*}{\partial y^{*2}}+e^{\varepsilon(4\xi_2-2\xi_3)}Ec\left(\frac{\partial^2\bar{\Psi}^*}{\partial y^{*2}}\right)^2+e^{-\varepsilon\xi_6}Q\theta^*, \tag{18}$$

$$e^{\varepsilon(\xi_1+\xi_2-\xi_3-\xi_7)}\left(\frac{\partial\bar{\Psi}^*}{\partial y^*}\frac{\partial\phi^*}{\partial x^*}-\frac{\partial\bar{\Psi}^*}{\partial x^*}\frac{\partial\phi^*}{\partial y^*}\right)=e^{\varepsilon(2\xi_2-\xi_7)}\frac{1}{Sc}\frac{\partial^2\phi^*}{\partial y^{*2}}-e^{-\varepsilon(m\xi_7)}K_r\phi^{*m}, \tag{19}$$

the boundary conditions are transformed as follows:

$$\frac{\partial\bar{\Psi}^*}{\partial y^*}=0,\ \frac{\partial\bar{\Psi}^*}{\partial x^*}=0,\ \theta^*=1,\ \phi^*=1\ \ at\ \ y^*=0,$$
$$\frac{\partial\bar{\Psi}^*}{\partial y^*}\to 0,\ \theta^*\to 0,\ \phi^*\to 0\ \ as\ \ y^*\to\infty. \tag{20}$$

The scaling group of transformations Γ, make system invariant if following parameters relation will hold

$$\xi_1+2\xi_2-2\xi_3=3\xi_2-\xi_3=-\xi_6=-\xi_7=\xi_2-\xi_3,$$
$$\xi_1+\xi_2-\xi_3-\xi_6=2\xi_2-\xi_6=4\xi_2-2\xi_3=-\xi_6,$$
$$\xi_1+\xi_2-\xi_3-\xi_7=2\xi_2-\xi_7=-m\xi_7,$$

by using elementary algebra, we get

$$\xi_2=\frac{1}{4}\xi_1=\frac{1}{3}\xi_3,\ \xi_4=\frac{1}{2}\xi_1,\ \xi_5=-\frac{1}{4}\xi_1,\ \xi_6=0,\ \xi_7=0,$$

thus resultant one-parameter group of transformations is given as:

$$\Gamma:\ x^*=xe^{\varepsilon\xi_1},\ y^*=ye^{\varepsilon\frac{\xi_1}{4}},\ \bar{\Psi}^*=\bar{\Psi}e^{\varepsilon\frac{3\xi_1}{4}},\ u^*=ue^{\varepsilon\frac{\xi_1}{2}},\ v^*=ve^{-\varepsilon\frac{\xi_1}{4}},\ \theta^*=\theta,\ \phi^*=\phi,$$

now expanding by Taylor's method up to $o(\varepsilon^2)$, we have

$$x^*-x=x\varepsilon\xi_1+o(\varepsilon^2),\ y^*-y=y\varepsilon\frac{\xi_1}{4}+o(\varepsilon^2),\ \bar{\Psi}^*-\bar{\Psi}=\bar{\Psi}\varepsilon\frac{3\xi_1}{4}+o(\varepsilon^2),$$

$$u^*-u=u\varepsilon\frac{\xi_1}{2}+o(\varepsilon^2),\ v^*-v=-v\varepsilon\frac{\xi_1}{4}+o(\varepsilon^2),\ \theta^*-\theta=0,\ \phi^*-\phi=0,$$

the associated characteristic equations are :

$$\frac{dx}{x\xi_1}=\frac{dy}{y\frac{\xi_1}{4}}=\frac{d\bar{\Psi}}{\bar{\Psi}\frac{3\xi_1}{4}}=\frac{du}{u\frac{\xi_1}{2}}=\frac{dv}{-v\frac{\xi_1}{4}}=\frac{d\theta}{0}=\frac{d\phi}{0}, \tag{21}$$

by solving Eq. (21), we get concerning similarity transformations:

$$\eta=x^{-\frac{1}{4}}y,\ \bar{\Psi}^*=x^{\frac{3}{4}}f(\eta),\ \theta^*=\theta,\ \phi^*=\phi, \tag{22}$$

using these values in Eqs. (17)-(19) under boundary conditions Eq. (20), ultimately we attain system of ordinary differential equations given as:

$$4f'''+3ff''-2f'^2+4Gr\theta Cos\alpha+4Gm\phi Cos\alpha+4(M+\frac{1}{K})f', \tag{23}$$

$$4\theta''+3\Pr f\theta'+4\Pr Ecf''^2+4\Pr Q\theta=0, \tag{24}$$

$$4\phi''+3Scf\phi'-4ScK_r\phi^m=0, \tag{25}$$

the transformed boundary conditions are given as:

$$f=0,\ f'=0,\ \theta=1,\ \phi=1\ \ at\ \ \eta=0,$$
$$f'\to 0,\ \theta\to 0,\ \phi\to 0\ \ as\ \ \eta\to\infty. \tag{26}$$

3 Numerical Scheme

The system of governing coupled non-linear ordinary differential Eqs. (23)-(25) subjected to endpoint conditions Eq. (26) have been solved by take on shooting method with fifth order R-K (Runge-Kutta) algorithm. The above mentioned highly non-linear ordinary differential equations with endpoints Eq. (26) are transformed into a first order system of equations. Let us suppose

$$l_2 = f',$$
$$l_3 = l'_2 = f'',$$
$$l_5 = \theta',$$
$$l_7 = \phi',$$

by introducing these new variables in Eqs. (23)-(25), we get

$$\begin{bmatrix} l'_1 \\ l'_2 \\ l'_3 \\ l'_4 \\ l'_5 \\ l'_6 \\ l'_7 \end{bmatrix} = \begin{bmatrix} l_2 \\ l_3 \\ \frac{1}{2}l_2^2 - \frac{3}{4}l_1 l_3 - (Grl_4 + Gml_6)Cos\alpha + \left(M + \frac{1}{K}\right)l_2 \\ l_5 \\ \Pr[-\frac{3}{4}l_1 l_5 - Ecl_3^2 - Ql_4] \\ l_7 \\ Sc[Cr(l_6)^m - \frac{3}{4}l_1 l_7] \end{bmatrix}, \quad (27)$$

we have seven new variables i.e $(l_1, l_2, l_3, l_4, l_5, l_6, l_7)$ than the endpoint conditions formulated under these variables as follows :

$$l_1(0) = 0,$$
$$l_2(0) = 0,$$
$$l_3(0) = unknown,$$
$$l_4(0) = 1, \quad (28)$$
$$l_5(0) = unknown,$$
$$l_6(0) = 1,$$
$$l_7(0) = unknown.$$

In order to integrate Eq. (27) as a IVP we require a values for $l_3(0)$ i.e. $f''(0)$, $l_5(0)$ i.e. $\theta'(0)$ and $l_7(0)$ implies $\phi'(0)$. Note that the initial conditions $l_3(0)$, $l_5(0)$, $l_7(0)$ are not given but we have additional endpoint conditions

$$l_2(\infty) = 0,$$
$$l_4(\infty) = 0, \quad (29)$$
$$l_6(\infty) = 0.$$

Choose favourable guess values for $f''(0)$, $\theta'(0)$ and $\phi'(0)$ so that the integration of system of first order differential equation carried out in such way the endpoint conditions in Eq. (29) hold absolutely. Step size $\Delta\eta = 0.09$ is used to find the numerical solution by four decimal accuracy as convergence criteria.

4 Results and Discussion

In this endorsement, investigations for the absolute insights of the physical model of the viscous incompressible, electrically conducting fluid embedded in a porous medium with high order chemical reaction effect has been carried out by using numerical approach. **Tables 1-6** and **Figs. 1-10** are provided to demonstrate the typical effects of physical parameters i.e magnetic parameter *M*, heat generation parameter *Q*, Prandtl number *Pr*, permeability parameter *K*, Eckert number *Ec*, Schmidt number *Sc*, temperature Grashof number *Gr*, species Grashof number *Gm*, chemical reaction parameter *Cr*, order of reaction *m*. The default parameter values for current computational analysis are given as *K* = 1.0, *Q* = 0.1, *M* = 1.0, *Ec* = 0.01, *Cr* = 0.5, $\alpha = 30^0$, *Gr* = 2.0, *Gm* = 2.0, *Pr* = 0.71 and *Sc* = 0.6, all graphic results corresponds to these values unless directed on the appropriate graphs.

Table 1. Numerical computations of $f''(0)$, $-\theta'(0)$ and $-\phi'(0)$ over *Gr*, *Gm*, *M* and *K* for *Ec* = 0.01, *Pr* = 0.71, *Cr* = 0.5, *Sc* = 0.6, *Q* = 0.

Gr	Gm	M	K	Reddy *et al.* [25] $f''(0)$	$-\theta'(0)$	$-\phi'(0)$	Present results $f''(0)$	$-\theta'(0)$	$-\phi'(0)$
2.0	2.0	1.0	1.0	1.67872	0.37536	0.632846	1.6761	0.3766	0.6304
3.0	2.0	1.0	1.0	2.06767	0.404755	0.648809	2.0278	0.4000	0.6418
4.0	2.0	1.0	1.0	2.44141	0.429506	0.66312	2.4066	0.4232	0.6602
2.0	3.0	1.0	1.0	2.03459	0.399334	0.646135	2.0585	0.3986	0.6408
2.0	4.0	1.0	1.0	2.38237	0.420826	0.658602	2.3959	0.4207	0.6501
2.0	2.0	2.0	1.0	1.49761	0.348147	0.619813	1.4838	0.3454	0.6137
2.0	2.0	3.0	1.0	1.36399	0.327933	0.610413	1.3087	0.3279	0.6184
2.0	2.0	1.0	2.0	1.49761	0.348174	0.619813	1.4833	0.3454	0.6137
2.0	2.0	1.0	3.0	1.36399	0.327933	0.610413	1.3083	0.3279	0.6114

Table 2. Numerical computations of $f''(0)$, $-\theta'(0)$ and $-\phi'(0)$ over *Pr, Ec* and *α* for *K* = 1.0, *Gr* = 2.0, *M* = 1.0, *Gm* = 2.0, *Sc* = 0.6, *Q* = 0.

Pr	Ec	α	Reddy *et al.* [25] $f''(0)$	$-\theta'(0)$	$-\phi'(0)$	Present results $f''(0)$	$-\theta'(0)$	$-\phi'(0)$
0.71	0.01	30^0	1.67872	0.37536	0.632846	1.6761	0.3766	0.6304
1.0	0.01	30^0	1.64902	0.429375	0.629509	1.6405	0.3297	0.6294
2.0	0.01	30^0	1.57721	0.570278	0.622038	1.5740	0.5748	0.6264
0.71	0.1	30^0	1.68425	0.337882	0.633256	1.6809	0.3327	0.6306
0.71	0.2	30^0	1.69051	0.29549	0.633719	1.6930	0.2906	0.6367
0.71	0.01	45^0	1.39653	0.352877	0.621139	1.3992	0.3540	0.6214
0.71	0.01	60^0	1.01526	0.318826	0.60434	1.0984	0.3161	0.6091

Table.3 Numerical computations of $f''(0), -\theta'(0)$ and $-\phi'(0)$ over *Sc and Cr* for *Ec= 0.01, Pr= 0.71, K*= 1.0, *Gr* = *Gm* = 2.0, *M*= 1.0, *α*= 30^0, *Q*= 0.

Sc	Cr	Reddy *et al.* [25] $f''(0)$	$-\theta'(0)$	$-\phi'(0)$	Present results $f''(0)$	$-\theta'(0)$	$-\phi'(0)$
0.5	0.5	_	_	_	1.6972	0.3801	0.5968
0.6	0.5	1.76872	0.37536	0.632846	1.6893	0.3777	0.6089
0.78	0.5	1.65106	0.369773	0.716312	1.6761	0.3763	0.6304
1.0	0.5	1.62341	0.364526	0.805778	1.6545	0.3647	0.7406
0.6	1.0	1.6253	0.36603	0.828406	1.6211	0.3628	0.8096
0.6	2.0	1.55591	0.355191	1.12767	1.6209	0.3620	0.8252

Table 4. Zeroth order missing slope for various values of *Q* and *Sc*.

Sc / **Q**	$-f''(0)$			$-\theta'(0)$			$-\phi'(0)$		
	0.22	0.62	0.78	0.22	0.62	0.78	0.22	0.62	0.78
0.0	1.1408	1.0846	1.0637	0.4204	0.4135	0.4109	0.4268	0.5885	0.6504
0.1	1.1562	1.1003	1.0794	0.3576	0.3500	0.3471	0.4274	0.5900	0.6522
0.2	1.1732	1.1175	1.0968	0.2902	0.2816	0.2784	0.4280	0.5916	0.6542
0.3	1.1920	1.1366	1.1160	0.2172	0.2076	0.2041	0.4286	0.5935	0.6565

Table 5. First order missing slope for various values of Q and *Sc*.

Sc / Q	$-f''(0)$			$-\theta'(0)$			$-\phi'(0)$		
	0.22	0.62	0.78	0.22	0.62	0.78	0.22	0.62	0.78
0.0	1.1510	1.1159	1.1040	0.4217	0.4175	0.4161	0.4028	0.5134	0.5531
0.1	1.1663	1.1313	1.1193	0.3591	0.3544	0.3528	0.4033	0.5148	0.5547
0.2	1.1832	1.1482	1.1363	0.2918	0.2865	0.2848	0.4039	0.5162	0.5565
0.3	1.2018	1.1669	1.1550	0.2190	0.2132	0.2112	0.4045	0.5178	0.5584

Table 6. Second order missing slope for various values of Q and *Sc*.

Sc / Q	$-f''(0)$			$-\theta'(0)$			$-\phi'(0)$		
	0.22	0.62	0.78	0.22	0.62	0.78	0.22	0.62	0.78
0.0	1.1549	1.1257	1.1156	0.4222	0.4187	0.4175	0.3921	0.4854	0.5190
0.1	1.1702	1.1409	1.1308	0.3596	0.3557	0.3543	0.3927	0.4868	0.5206
0.2	1.1870	1.1577	1.1475	0.2924	0.2879	0.2864	0.3932	0.4882	0.5223
0.3	1.2056	1.1762	1.1661	0.2197	0.2147	0.2130	0.3939	0.4899	0.5243

The effects of physical parameters over skin friction coefficient, wall temperature and wall concentration gradient are numerically obtained and presented through **Tables 1-3**. It has found from **Table 1** that the skin friction coefficient, wall temperature gradient i.e. heat transfer rate and wall concentration gradient i.e. mass transfer rate increases for higher values of thermal and solutal Grashof number. Whereas the skin friction coefficient, Nusselt and Sherwood number shows opposite comportment against increasing values of M (magnetic parameter) and K (permeability parameter). **Table 2** shows that the heat transfer rate decreases for higher values of Eckert number Ec and inclination α, while it shows increasing behavior for increasing values of Prandtl number Pr. **Table 3** indicates that the mass transfer rate increasing as chemical reaction parameter Cr and Schmidt number Sc increases. Progressive values of the buoyancy parameters that is thermal Grashof number ($Gr > 0$) and solutal Grashof number ($Gm > 0$) are reported. $Gr > 0$ relates to cooling of plate, whereas $Gm > 0$ implies that the concentration of chemical species in the free stream regime is less then the concentration at the endpoint surface. **Fig. 1** paints the influence of permeability parameter K on both velocity and temperature distribution. It has been observed that throughout the boundary layer regime by increasing permeability parameter K velocity profile decreases and the presence of porous media creates huge resistance to fluid flow due to which trifling changes occurs in momentum boundary layer and hence inciting of fluid temperature appeared. The response of temperature and velocity profiles for various values of heat generation parameter Q is depicted in **Fig. 2**. Temperature profile is effected significantly and increases against larger values of heat generation parameter $Q > 0$. Higher values of the Q (heat generation parameter) generates energy which results enhancement of velocity. Infect, this change (increase) in the average kinetic energy produces an increment in the flow field velocity due to buoyancy effect. Influence of applied magnetic field on flow field is reported in **Fig. 3**. It is found that magnetic field has a prominent reducing effect on the velocity profile. This fact is due to retarding-type force i.e Lorentz force because application of transverse magnetic field perpendicular to the x-axis along which fluid flow is assumed give rise to Lorentz force, which has tendency to deaccelerate fluid particles and hence velocity profile decreases. **Fig. 3** also shows that temperature profile increases for magnetic parameter M. For higher values of magnetic parameter M, magnitude of Lorentzian retardation increases so work has been done by fluid to overcome this resistive force and this supplementary work is then dissipated as a thermal energy which is the source so that the fluid to be heated in a boundary layer and hence temperature increases. From figure it is also perceived that the counter-productive effect of heating the viscous fluid is on a serious node therefore, to achieve flow regulation, to avoid excessive temperatures and growth of the thermal boundary and to explore the desired fluid characteristics, intelligent use of magnetic field is required. The viscous dissipation parameter i.e. Ec (Eckert number) the addition of heat due to viscous dissipation and is equal to 0.01 for incompressible fluids i.e $\nabla\cdot V=0$. Influence of Eckert number Ec over temperature and velocity profiles is sketched in **Fig. 4** and it is evident that in the presence of heat source parameter the viscous dissipation leads to increase in temperature profile.

The positive values of *Ec* indicates cooling of plate that is, loss of heat from the surface to the fluid so that the greater values of viscous dissipative heat cause enhancement of temperature and velocity profile as well. In addition, it has been seen that magnitude of the thermal boundary layer is significantly large under viscous dissipation effect. The effects of chemical reaction parameter *Cr* on the temperature and velocity profile are analyzed in **Fig. 5**. It shows that the temperature profile increases throughout the boundary layer regime, due to increasing values of chemical reaction parameter *Cr*. Since chemical energy is converted into thermal energy which results fluid warmness. Whereas, the velocity profile decreases across the boundary layer by increasing *Cr*.

Fig. 6 is plotted to examine the influence of acute angle α on velocity distribution. Vertical surface produce inciting attitude in velocity as compare to inclined surface. This is due to buoyancy effect because the plate is inclined and have gravity component cosα. So that higher values of inclination, the productive involvement of buoyancy force falls by a factor of cosα. Ultimately the driven force for the fluid reduces which yields decrease in velocity profile. Physical interpretation of thermal Grashof number *Gr* is assinged via **Fig. 7**. The comparative influence of the thermal buoyancy force towards viscous hydro- dynamic force signifies by thermal Grashof number *Gr*. So increase in *Gr* means increment in thermal buoyancy force in a flow regime which results increase in velocity profile. It has been observed from **Fig. 7** there is a sharp evolution in the velocity near the porous surface. The velocities shoots towards extreme and then decays properly to zero far from the plate. We observed that the monotonically decrease of velocities from peak values to the free stream zero satisfying the far field endpoint conditions. The effect of solutal Grashof number *Gm* over velocity profile is given by **Fig. 8**. It is seen that larger values of solutal Grashof number *Gm* brings increase in velocity profile within a boundary layer.

Fig. 9 is used to examine the impact of Prandtl number *Pr* over temperature distribution. Prandtl number *Pr* has inverse relation with thermal conductivity so from physical point of view it is clear that the lager Prandtl number reflects weaker thermal diffusivity and hence thinner thermal boundary layer. Whereas, it is also observed that the temperature profile increases for high order chemical reaction m. **Fig. 10** is sketched to explore the behavior of Schmidt number *Sc* and high order chemical reaction m. It is evident that the concentration profile decreases for higher values of Schmidt number *Sc*. For higher values of Schmidt number *Sc* concentration buoyancy effects reduces which yields decrease in the flow velocity. Further, Schmidt number *Sc* is the ratio of the momentum to the mass diffusivity so the relative influence of momentum diffusion to species diffusion is signifies by Schmidt number. When *Sc* is unity it mean both momentum and species will diffuse at equal rate in the flow regime. Under this case both momentum and concentration boundary layer will be of same order of magnitude. Note that for *Sc* > 1 diffusion of momentum will be faster than that of species diffusion and for *Sc* < 1 diffusion of species overcome momentum diffusivity. The influence of order of chemical reaction over concentration profile is depicted in **Fig. 10** as well.

The concentration profile increases as order of chemical reaction increases i.e *m* = 0, *m* = 1, *m* = 2. **Tables 4-6** recapitulated the numerical computations of skin friction coefficient, heat and mass transfer rate for zeroth, first and second order chemical reaction over $0.22 \leq Sc \leq 0.78$. It is concluded that the skin friction coefficient increases whereas heat transfer rate decreases for increasing values of heat generation parameter *Q*. Whereas, there is a trifling increase in mass transfer rate against heat generation parameter *Q*. It is also observed that the skin friction coefficient and heat transfer rate exhibit greater values in case of hydrogen i.e *Sc* = 0.22 than that of water vapour (*Sc* = 0.62) and NH_3 i.e *Sc* = 0.78. Whereas, mass transfer rate show greater values for NH_3 as compare to hydrogen and water vapour, for *K* = 1.0, *Gr* = 2.0, *M* = 1.0, *Gm* = 2.0, *Pr* = 0.71, $\alpha = 30^0$, *Ec* = 0.01, *Cr* = 0.5.

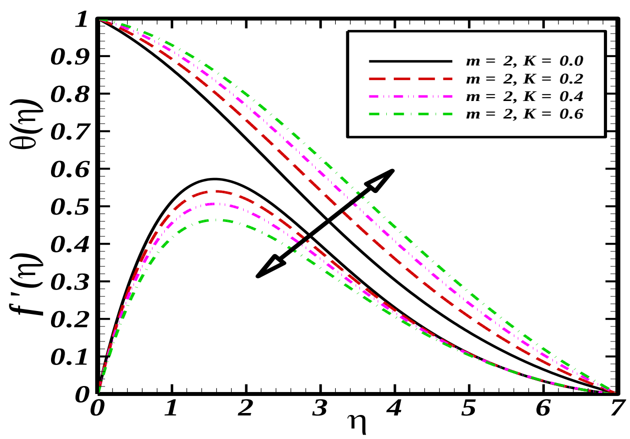

Fig. 1. Influence of curvature parameter *K* on velocity and temperature distribution.

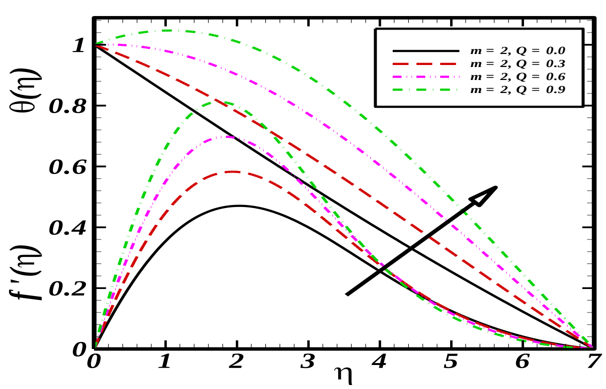

Fig. 2. Influence of heat generation parameter *Q* on velocity and temperature distribution.

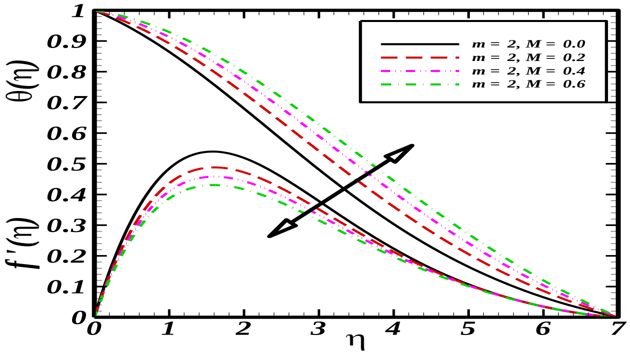

Fig. 3. Influence of magentic parameter *M* on velocity and temperature distribution.

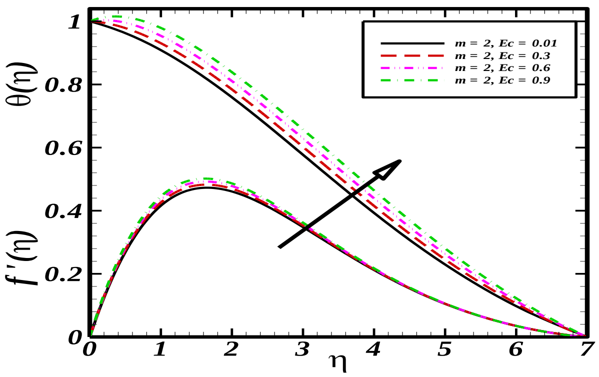

Fig. 4. Influence of Eckert number *Ec* on velocity and temperature distribution.

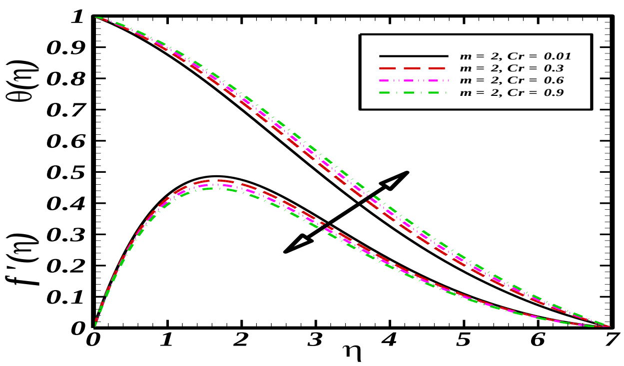

Fig. 5. Influence of chemical reaction parameter *Cr* on velocity and temperature distribution.

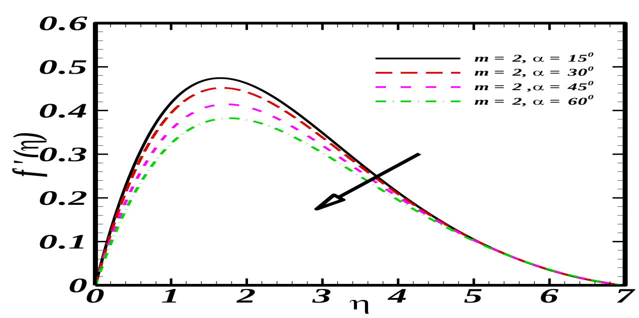

Fig. 6. Influence of inclination α on velocity distribution.

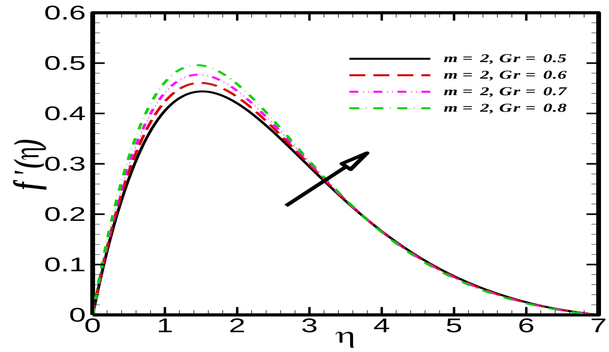

Fig. 7. Influence of thermal Grashof number *Gr* on velocity distribution.

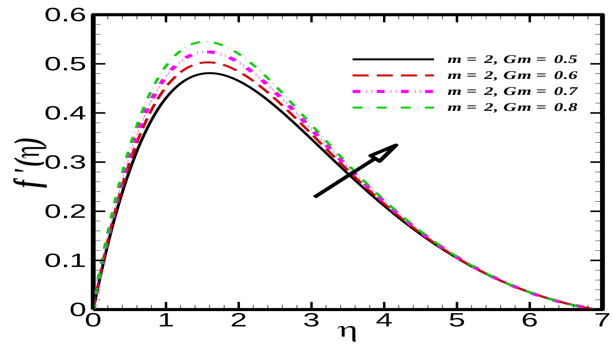

Fig. 8. Influence of solutal Grashof number *Gm* on velocity distribution.

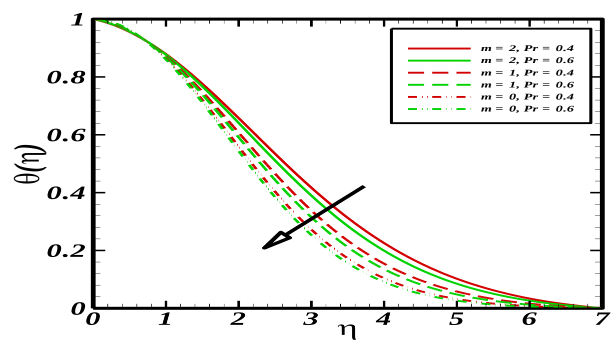

Fig. 9. Influence of Prandtl number *Pr* and order of chemical raeaction *m* on temperature distribution.

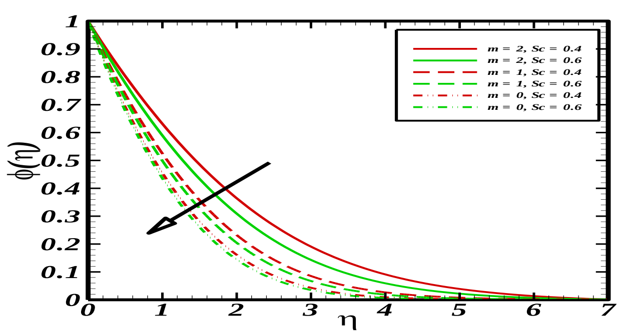

Fig. 10. Influence of Schmidt number *Sc* and order of chemical raeaction *m* on concentration distribution.

5 Concluding Remarks

The present computational analysis helps us to understand physically the natural convection two dimensional steady incompressible, chemically reacting viscous fluid flow past over a porous plate in the presence of heat generation and viscous dissipation. Due to non-linearity factor, it is not a easy task to solve governing equations of motion to get complete physical description. Method of Lie group analysis has been adopted to tackle the difficulties appears in solving partial differential equations of motion. We determined the Lie group transformations under which the governing partial differential equations and associated endpoints conditions remain invariant and similarity variables are obtained through relative symmetries for current flow model which has extreme applications regarding practical engineering disciplines especially in the field of fluid mechanics. Ultimately reduction of independent variable generates system of ordinary differential equations and this system is solved by using fifth order R-K (Runge-Kutta) algorithm with shooting technique. The main finding results regarding physical interest of this investigation on velocity, temperature and concentration profiles are itemized as follows:

1) The effect of permeability parameter K on fluid flow is to suppress the velocity of fluid, which in turn to yields significant enhancement of temperature profile.
2) Temperature and velocity profile effected considerably towards buoyancy effect and both increases when heat generation parameter Q increases.
3) Application of transverse magnetic field has substantial effect over the flow field. An increase in magnetic parameter M brings retardation in flow field velocity at all points while opposite attitude is observed in case of temperature distribution.
4) Higher values of viscous dissipation parameter Ec leads to significant increase in temperature and velocity profiles.
5) The velocity profile decreases across the boundary layer while temperature profile increasing throughout the flow regime against higher values of chemical reaction parameter Cr .
6) The impact of increasing values of thermal Grashof number Gr and solutal Grashof number Gm is manifested as an increase in fluid velocity. Whereas, fluid velocity decreases by increasing inclination α of the plate.
7) As expected, temperature flow profile decreases for higher values of Prandtl number Pr while it is found that the temperature profile increases for high order chemical reaction m.
8) The concentration flow profile decreases gradually as the Schmidt number Sc increases. Whereas, it shows increasing behaviour for high order chemical reaction m.
9) It is perceived that the skin friction coefficient and heat transfer rate shows inciting attitude in the case of hydrogen than that of water vapour and NH_3. Interestingly, mass transfer rate exhibit greater values for NH_3 as compare to hydrogen and water vapour.
10) Skin friction coefficient, heat and mass transfer rate are compared with that of Reddy *et al.* [25]. This aids to stability and conformity of the present analysis.

References

[1] L.V. Ovsiannikov, Group Analysis of Differential Equations, Academic Press, New York (1982).

[2] P.J. Olver, Application of Lie Groups to Differential Equations, Springer, Berlin (1986).

[3] G.W. Bluman, S. Kumei, Symmetries and Differential Equations, Springer, New York (1989).

[4] N.H. Ibragimov, Elementary Lie Group Analysis and Ordinary Differential Equations,

Wiley, New York (1999).

[5] M. Pakdemirli, M. Yurusoy, Similarity transformations for partial differential equations, SIAM Rev. 40, 96-101 (1998).

[6] M. Yurusoy, M. Pakdemirli, Symmetry reductions of unsteady three-dimensional boundary layers of some non-Newtonian fluids, *International Journal of Engineering Science.* 35, 731-740 (1997).

[7] V.K. Kalpakides, K.G. Balassas, Symmetry groups and similarity solutions for a free convective boundary-layer problem, *International Journal Non-linear Mechanics*. 39, 1659-1970 (2004).

[8] H.S. Hassan, S.A. Mahrous, A. Sharara, and A. Hassan, A Study for MHD Boundary

Layer Flow of Variable Viscosity over a Heated Stretching Sheet via Lie-Group Method. *Applied Mathematics and Information Sciences*, in Press (2014).

[9] S. Sivasankaran, M. Bhuvaneswari, P. Kandaswamy, E.K. Ramasami, Lie group analysis of natural convection heat and mass transfer in an inclined surface, *Nonlinear Analysis Modelling and Control.* 11, 201-212 (2006).

[10] N. Beithou, K. Albayrak, and A. Abdulmajeed, Effects of porosity on the free convection flow of non- Newtonian fluids along a vertical plate embedded ina porous medium, *Turkish Journal of Engineering and Environmental Science.* 22, 203-209 (1998).

[11] C.H. Chen, Heat and mass transfer in MHD flow by natural convection from a permeable, inclined surface with variable wall temperature and concentration, *Acta Mechanica*. 172, 219-235 (2004).

[12] Anjali Devi, B. Ganga, Viscous dissipation effect on non-

linear MHD flow in a porous medium over a stretching porous surface, *International Journal Applied Mathematics Mechanics.* 5, 45-59 (2009).

[13] M. Turkyilmazoglu, Multiple solutions of heat and mass transfer of MHD slip flow for the viscoelastic fluid over a stretching sheet, *International Journal of Thermal Sciences.* 50, 2264-2276 (2011).

[14] S.V. Subhashini, N. Samuel, I. Pop, Double-diffusive Convection from a Permeable Vertical Surface under Convective Boundary Condition, *International Communications* in *Heat* and *Mass* Transfer. 38, 1183-1188 (2011).

[15] T. Hayat, Z. Iqbal, M. Qasim, S. Obaidat, Steady Flow of an Eyring Powell Fluid over a Moving Surface with Convective Boundary Conditions, *International Journal of Heat and Mass Transfer*. 55, 1817-1822 (2012).

[16] M.G Reddy, Scaling Transformation for Heat and Mass Transfer Effects on Steady MHD Free Convection Dissipative Flow Past an Inclined Porous Surface, *International Journal Applied Mathematics Mechanics.* 9, 1-18 (2013).

[17] M.C. Raju, S.V.K. Varma, B. Seshaiah, Heat transfer effects on a viscous dissipative fluid flow past a vertical plate in the presence of induced magnetic field, *Ains Shams Engineering Journal.* 6, 333-339 (2015).

[18] R. Kandasamy, K. Periasamy, KK.P. Sivagnana, Chemical reaction, heat and mass transfer on MHD flow over a vertical stretching surface with heat source and thermal stratification effects, *International Journal Heat Mass Transfer*. 48, 4557-4561(2005).

[19] Mingchun Lia, Yusheng Wua, Yanwen Tianb, Yuchun Zhaib, Non-thermal equilibrium model of the coupled heat and mass transfer in strong endothermic chemical reaction system of porous media, *International Journal Heat Mass Transfer.* 50, 2936-2943 (2007).

[20] N. Kishan, P. Amrutha, Effects of Viscous Dissipation on MHD Flow with Heat and Mass Transfer over a Stretching Surface with Heat Source, Thermal Stratification and Chemical Reaction, *Journal of Naval Architecture Marine Engineering.* 7, 11-18 (2011).

[21] R. Kandasamy, T. Hayat, S. Obaidat, Group theory transformation for Soret and Dufour effects on free convective heat and mass transfer with thermophoresis and chemical reaction over a porous stretching surface in the presence of heats source/sink, *Nuclear Engineering and Design*. 241, 2155-2161 (2011).

[22] O.D. Makinde, P. Sibanda, Effects of chemical reaction on boundary layer flow past a vertical stretching surface in the presence of internal heat generation, *International Journal of Numerical Fluid Flows*, In press. 2, 89-94 (2012).

[23] R.S. Tripathy, G.C. Dash, S.R. Mishra, S. Baag, Chemical reaction effect on MHDfree convective surface over a moving vertical plate through porous medium, *Alexandria Engineering Journal*. 54, 673-679 (2015).

[24] M. Ferdows, Al-Mdallal, M. Qasem, Effects of Order of Chemical Reaction on a Boundary Layer Flow with Heat and Mass Transfer Over a Linearly Stretching Sheet, *American Journal Of Fluid Dynamics*. 2, 89-74 (2012).

[25] G.V.R. Reddy, S.M. Ibrahim, V.S. Bhagavan, Similarity transformations of heat and mass transfer effects on steady MHD free convection dissipative fluid flow past an inclined porous surface with chemical reaction, *Journal of Naval Architecture Marine Engineering*. 11, 157-166 (2014).

M.Y. Malik is Professor at Quaid-i-Azam University Islamabad. He received PhD degree in Mathematics (2000) from Department of Mathematics, University of Bradford, England (UK). He has published many papers in the area of computational fluid dynamics. He is referee of different mathematical journals.

Khalil Ur Rehman is working as a research scholar in department of mathematics at Quaid-i-Azam University Islamabad, Pakistan under the supervision of Dr. M.Y. Malik. His research interests are in computational fluid dynamics and Lie symmetry analysis of differential equations.